

GEOCHEMICAL CHARACTERISATION OF QUARTZ LATITE UNITS IN THE ETENDEKA FORMATION

S.C. Milner and A.R. Duncan

Department of Geochemistry, University of Cape Town, Rondebosch 7700

ABSTRACT

Quartz latite units interbedded with basaltic lavas in the Etendeka Formation form extensive sheet-like deposits which are probably the product of high temperature ash-flows. Apart from some systematic differences between pitchstone and devitrified quartz latites, largely explained by low temperature alteration processes, individual quartz latite units exhibit remarkably uniform compositions. No significant lateral compositional variations within individual units are observed and compositional changes occur only in the uppermost parts of any particular unit. A regional stratigraphic correlation is difficult to establish due to local differences that may be attributed to palaeotopography and the faulted nature of the coastal region in the Etendeka. In this study geochemistry has been used as a primary criterion for the correlation of major quartz latite units within the southern Etendeka area.

1. INTRODUCTION

The geology of the Etendeka region in S.W.A/Namibia has been described in some detail by Erlank *et al.* (1984) and Milner (1986). In summary, the Etendeka Formation consists of a series of interbedded basalt and quartz latite units which overlie Karoo sediments and pre-Karoo basement. Detailed mapping of the southern Etendeka area (Milner, 1986) has shown that the quartz latites, which form extensive sheet-like deposits but rarely exhibit pyroclastic textures, are probably high-temperature ash flow tuffs. Three distinct groups of quartz latite units are recognised in the field by differences in outcrop pattern and petrographic character, namely the Springbok, Tafelberg and Interbedded Coastal groups. The term "unit" as used here can be considered synonymous with "cooling unit". It is not certain whether some cooling units contain multiple flow units, but this would seem likely in some areas on the basis of outcrop characteristics.

Recent field studies have resulted in a refinement of the stratigraphy defined by Milner (1986). A section through the Springbok group south of the Huab River has revealed the presence of a second lower Springbok quartz latite unit and two additional quartz latite units have been recognised in the Tafelberg group. The first of the additional Tafelberg quartz latites is a thin, sparsely porphyritic unit cropping out 15-20 m below the upper Tafelberg unit between Wêreldsend and Bergsig, and will be referred to as the middle Tafelberg unit. The second is a separate unit above the main upper Tafelberg quartz latite which was sampled at Tafelberg beacon and will be referred to as the Tafelberg beacon unit. A regional stratigraphic column for the Etendeka Formation is not readily compiled using the field and petrographic data available because of local differences in stratigraphy and the faulted nature of the coastal region.

A total of 198 quartz latite samples have been analysed for 32 major and trace elements and it is now possible to attempt a chemical characterisation of individual quartz latite units. This characterisation en-

ables a stratigraphic correlation of units where field and petrographic relationships are obscure. The effects of primary within-unit variation and secondary alteration have also been taken into consideration. In all of the diagrams the data presented were not recalculated to 100% on a volatile free basis.

2. CLASSIFICATION OF QUARTZ LATITES

Erlank *et al.* (1984) divided the acidic rocks of the Etendeka Formation into quartz latites and high K dacites on the basis of their relative SiO_2 and K_2O contents, according to the classification schemes proposed by MacKenzie and Chappell (1972) and Peccerillo and Taylor (1976). Only three of the Etendeka acidic rocks were classified as high-K dacites with markedly lower K_2O contents than the quartz latites. All the presently analysed Etendeka acidic rocks are plotted on a SiO_2 vs K_2O diagram (Fig. 1).

With the much larger data set that is now available it is clear that all samples with lower K_2O contents, and specifically those which plot in the dacite or high K-dacite fields, are pitchstones. Most of the acid rocks

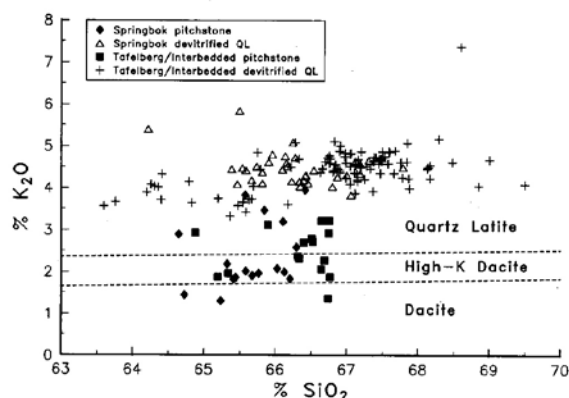


Fig. 1: K_2O - SiO_2 variations in acidic rocks (pitchstones and devitrified quartz latites) of the Etendeka Formation. The classification boundaries are from MacKenzie and Chappell (1972). The "Tafelberg/Interbedded devitrified QL" includes samples from all Tafelberg and all Interbedded Coastal quartz latite units.

have a cryptocrystalline to microcrystalline groundmass in which devitrification textures are common and such rocks will be referred to in this paper as devitrified quartz latites.

The pitchstones whose compositions are shown in Fig. 1 are from a variety of localities and units. The pitchstones generally crop out at the Base of a unit (see Milner, 1986, Fig. 3) but there are rare instances where pitchstone also forms lenses or bands within the main body of a unit. Pitchstone and devitrified quartz latite are often found in close proximity at the same stratigraphic height near the base of a unit. No examples are known of a low-K (< 3.0 per cent K₂O) devitrified quartz latite in the Etendeka Formation. Therefore, it seems unlikely that the pitchstones represent a distinct magma type, or an eruptive product from a compositionally zoned magma chamber which was also the source of the devitrified quartz latites.

3. QUARTZ LATITE ALTERATION

Comparison of whole-rock data for pitchstone and devitrified quartz latite pairs from the upper Springbok and lower Interbedded Coastal groups are presented in Table 1. The samples in each pair, which were collected at similar locations and heights within each unit,

TABLE 1: A Comparison of individual pitchstone and devitrified quartz latite sample pairs.

	Upper Springbok		Lower Interbedded Coastal	
	Pitchstone Sample (SM23)	Devitrified Sample (SM21)	Pitchstone Sample (SM97)	Devitrified Sample (SM98)
SiO ₂	65.68	66.42	66.34	67.68
TiO ₂	0.91	0.92	0.84	0.86
Al ₂ O ₃	12.63	12.61	12.81	12.98
Fe ₂ O ₃ *	6.65	6.89	5.72	5.82
MnO	0.11	0.15	0.11	0.08
MgO	1.11	1.50	0.97	1.15
CaO	3.73	2.58	3.15	2.35
Na ₂ O	3.27	2.50	3.54	2.83
K ₂ O	1.91	4.28	2.32	4.89
P ₂ O ₅	0.27	0.27	0.28	0.28
H ₂ O-	0.64	0.36	0.25	0.13
LOI	3.12	1.39	3.45	1.11
TOTAL	100.03	99.87	99.75	100.16
Cs	28	< 5	19.5	< 5
Rb	196	166	191	184
Ba	657	638	648	612
Sr	186	147	160	132
Zr	269	265	266	267
Nb	22	23	25	24
V	65	67	55	60
Cu	14.4	13.4	38	42
Y	42	44	42	41
La	46	46	44	44
Ce	90	91	87	85
Nd	47	50	48	47

Fe₂O₃ * - Total Fe reported as Fe₂O₃.

LOI - Loss of volatiles after roasting at 850°C

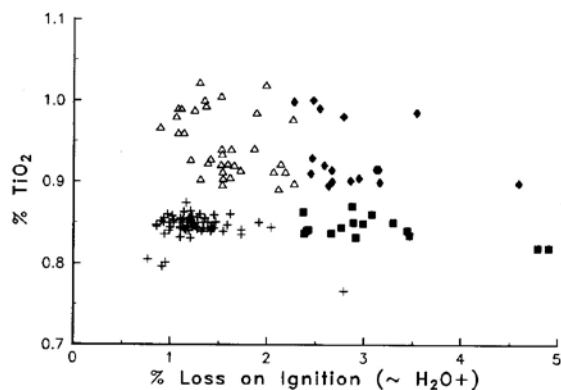
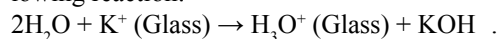


Fig. 2: Variation of LOI as a function of textural variety in acidic rocks of the Etendeka Formation. Note that pitchstones always show > 2.2 per cent LOI and that there is little difference in the TiO₂ content of pitchstones and devitrified quartz latites from the same units. See Fig. 1 for legend. Data for the upper Tafelberg, and the middle and upper Interbedded Coastal quartz latite units are not shown on this figure as no pitchstones from those units have been analysed.

show differences for a number of oxides and elements, but particularly for K₂O, LOI, CaO, Na₂O and Cs. The juxtaposition of sample sites suggests that these differences are not of a primary magmatic nature and may reflect secondary alteration processes. Elements considered relatively immobile during alteration support this conclusion, as illustrated by a plot of TiO₂ vs. LOI (Fig. 2). This figure also indicates that simple addition or subtraction of H₂O+ (the dominant component of LOI) cannot account for the compositional variations observed.

Petrographically the pitchstones appear unaltered and it is tempting to regard their composition as that most closely representing the original quartz latite magma. However, they represent a small proportion of the quartz latite outcrop in the Etendeka area and it seems highly unlikely that the main volume of devitrified quartz latite, totalling several hundred cubic kilometres, could gain up to 2 wt per cent K₂O by post-eruptive alteration in a subaerial environment. Zielinski (1982), Jezek and Noble (1978) and Cerling *et al.* (1985) have documented alkali exchange and loss in volcanic glass and reported that a low temperature hydration of glass by ground water is accompanied by the exchange of Na⁺ and K⁺ with positive hydronium ions (H₃O⁺) in the following reaction:



Cerling *et al.* (1985) stated that in peralkaline glasses "up to 40 per cent of the alkali cations (Na⁺ and K⁺) could be replaced by H⁺ with no measurable change in the bulk composition of the glass or in the distribution of minor and trace elements, excepting other alkali ions such as Rb⁺".

A plot of K₂O against LOI for the Etendeka samples exhibits a negative correlation, which is consistent with alkali loss during a hydration event (Fig. 3a). This relationship is more clearly illustrated by a plot of K₂O/LOI

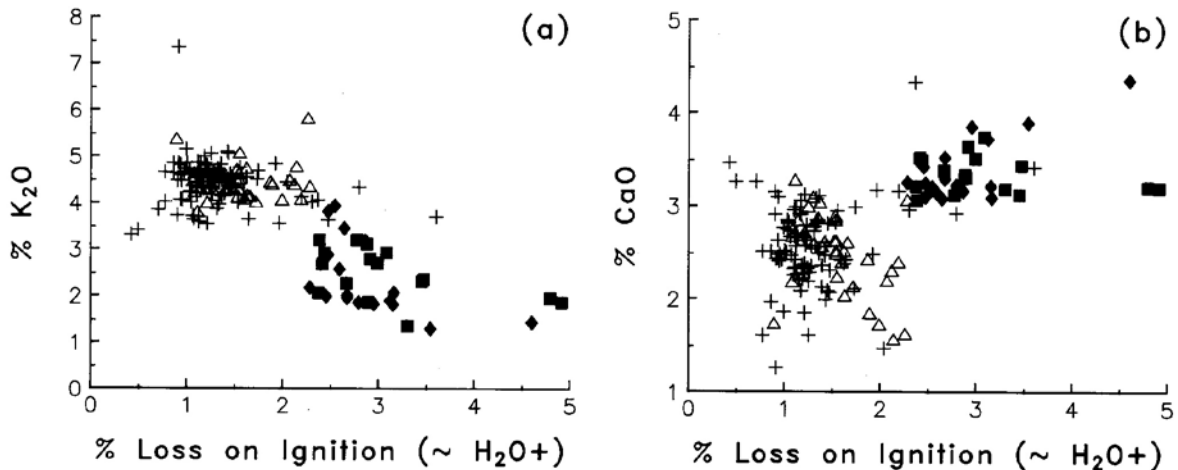


Fig. 3: Variation of K_2O and CaO as a function of the LOI of devitrified quartz latites and pitchstones from the Etendeka Formation. See Fig. 1 for legend.

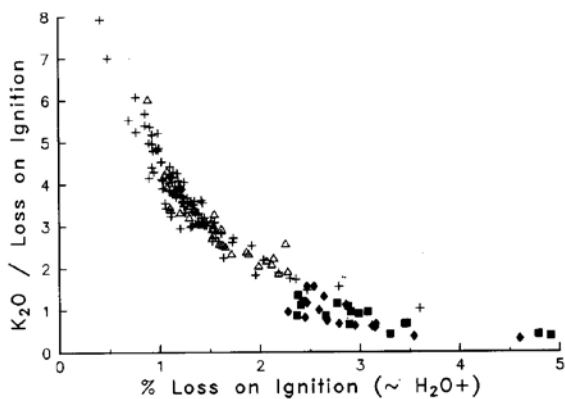


Fig. 4: Plot of the ratio K_2O/LOI against LOI for devitrified quartz latites and pitchstones from the Etendeka Formation. See Fig. 1 for legend.

against LOI (Fig. 4). The relative magnitude of K_2O and LOI variations shown in Fig. 3a and the well-defined trend in Fig. 4 strongly suggest that $H_2O +$ is the principle exchange component for K^+ in the glass. It is surprising, however, that pitchstones and devitrified quartz latites do not show different concentrations of Rb and that pitchstones appear to have markedly higher concentrations of Na_2O and Cs than do the devitrified quartz latites (Table 1).

The higher concentration of CaO in the pitchstones relative to the devitrified quartz latites (Fig. 3b) is more difficult to explain. Since Al_2O_3 contents in the pitchstones and devitrified quartz latites do not differ significantly, differences in CaO cannot be ascribed to preferential concentration of plagioclase phenocrysts in the pitchstones. Plagioclase and pyroxene crystals in the pitchstones show little alteration compared to those in the devitrified quartz latites, which are often replaced by sericite, serpentine and minor carbonate. It seems likely that as a consequence of this alteration process CaO_1 and possibly Na_2O_1 has been lost from the devitri-

fied quartz latites.

In conclusion, the alkali and alkali earth elements are mobile in post-eruptive alteration processes and the concentrations of these elements are not representative of primary eruptive compositions. This is an important factor to consider in petrogenetic modelling and has serious implications for K-Ar and Rb-Sr age dating techniques.

4. WITHIN-UNIT VARIATION

Detailed studies of many ash flow deposits that are related to calderas show systematic mineralogical and chemical variations, as exemplified by the Bishop Tuff, California (Hildreth, 1979), the Bandelier Tuff, Valles Caldera, New Mexico (Smith and Bailey, 1966) and the Mazama ash flow, Crater Lake, Oregon, (Williams, 1942; Ritchey, 1980). Vertical zonations within ash flows are often translated into lateral variations as the sheet thins away from its source area. It is necessary therefore to recognise such trends if successful correlations are to be made in distal or faulted portions of a succession. Processes leading to within-flow variation include sorting (which may involve crystal-glass fractionation during eruption and outflow), alteration, and pre-eruptive compositional gradients in magma chambers. Hildreth (1981) and Smith (1979) gave comprehensive accounts of the types of compositional zonations observed in ash-flow tuffs and suggested possible mechanisms for their formation.

Serial stratigraphic sections and lateral traverses were sampled in several localities in order to evaluate the extent to which the Etendeka quartz latites show vertical and lateral variations. The discussion below is specific to a single quartz latite unit but identical conclusions can be drawn from comparable studies made on other quartz latite units.

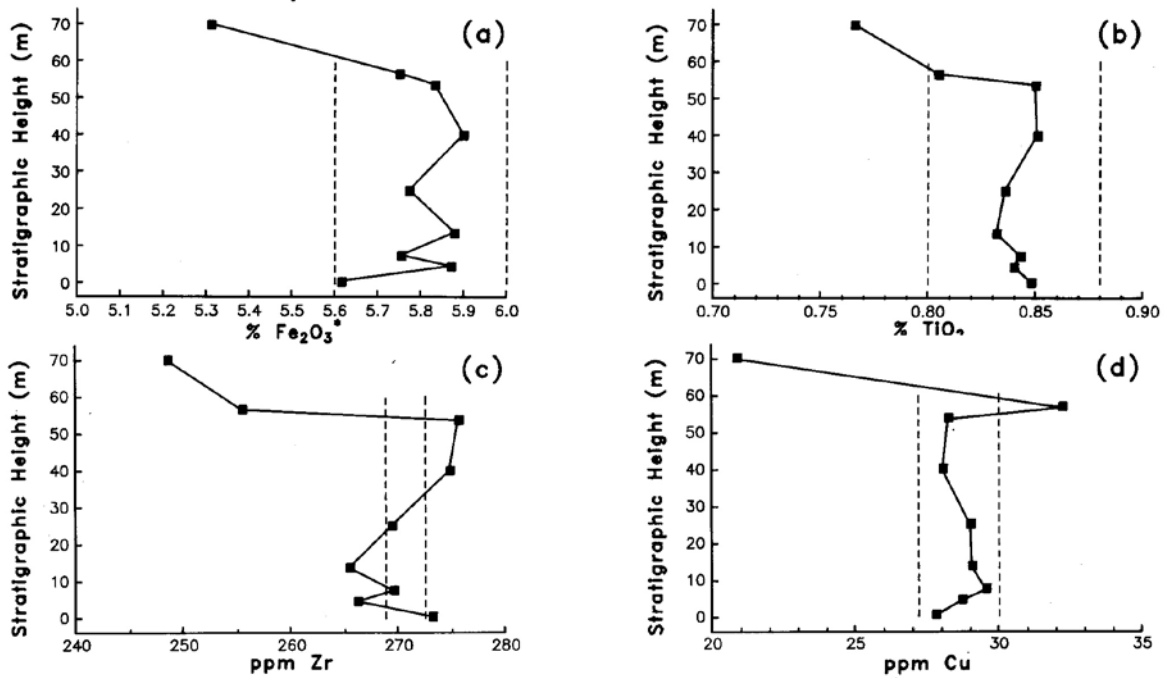


Fig. 5: Variation in the concentration of Fe₂O₃* (total Fe expressed as Fe₂O₃), TiO₂, Zr and Cu as a function of stratigraphic height within the lower Tafelberg quartz latite unit in a single section on the farm Wêreldsend. The dashed vertical lines represent 2 sigma analytical errors added and subtracted to the mean of the lowermost 7 samples in the section. For Fe₂O₃* and TiO₂ the errors are estimated from 6 replicate analyses, for Zr and Cu they are estimated from XRF counting statistics only.

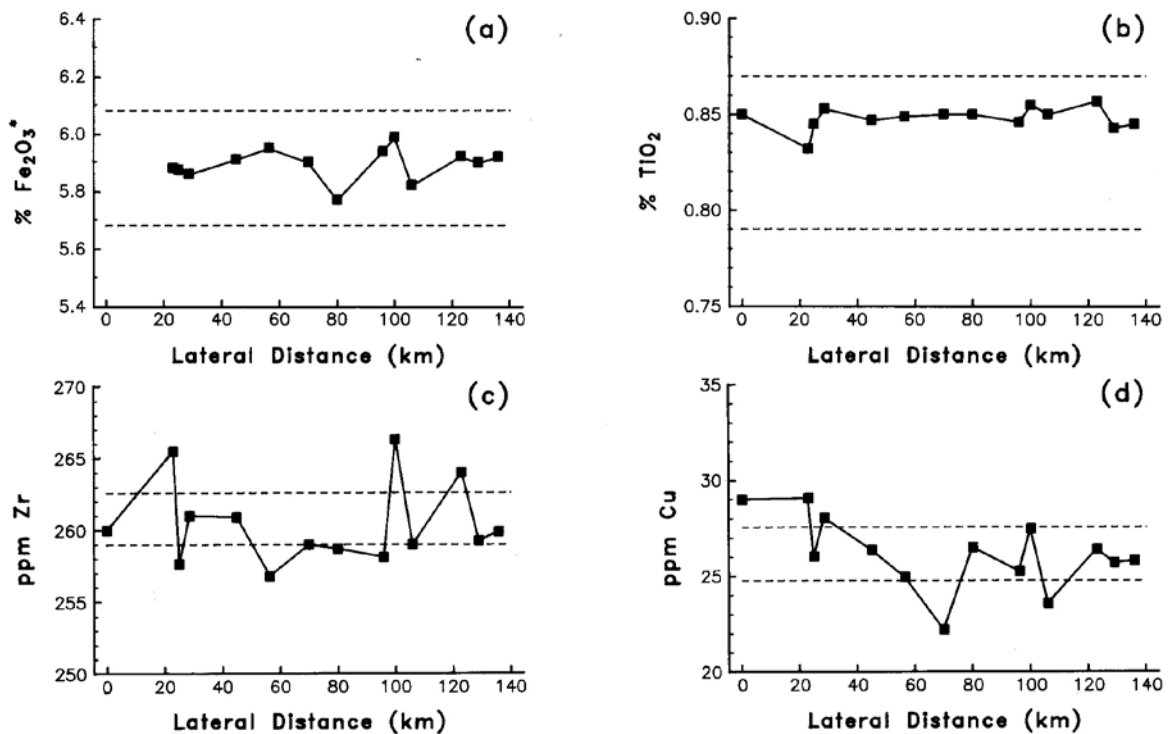


Fig. 6: Variation in the concentration of Fe₂O₃*, TiO₂, Zr and Cu as a function of lateral distance within the lower Tafelberg quartz latite. The section runs from Tafelberg (0 km) eastwards in the vicinity of the Bergsig - Torra Bay road to the Ambrosius Berg Fault Zone (80 km) and then southwards along strike to Ambrosius Berg (140 km). The dashed horizontal lines represent 2 sigma analytical errors added and subtracted to the mean of all samples in the traverse.

4.1 Vertical Variation

The evidence for vertical compositional variation within the quartz latite units can be illustrated using the lower Tafelberg unit as a type example. A 70 m section of this unit was sampled on the farm Wêreldsend, where the exposure is complete and readily accessible. Fig. 5 shows the variation of Fe_2O_3^* , (total iron reported as Fe_2O_3) TiO_2 , Zr and Cu with height from the base. These elements are not affected by the alteration processes discussed above and also show the greatest differences between different quartz latite groups and units (see Section 5). Within the main body of the unit (0-65 m) Fe_2O_3 , TiO_2 , Zr and Cu show no systematic variation outside the limits of analytical error. However, the two uppermost samples show significant departures from the composition of the lower portions of the unit. This is probably due to high temperature alteration where the contorted, brecciated and amygdaloidal flow top is highly oxidised and contains abundant zeolite and secondary quartz.

4.2 Lateral Variation

The limited range of compositions exhibited within a vertical section allows the construction of a lateral traverse with samples that are not necessarily from the same stratigraphic level within an individual unit. A traverse of this nature was constructed for the lower Tafelberg unit from isolated hilltop remnants between Tafelberg in the east and the more tilted succession in the west. West of the Ambrosius Berg Fault Zone, where the lower Tafelberg unit is down-faulted, samples were collected along strike between the Torra Bay-Bergsig road and Ambrosius Berg (See Fig. 2 in Milner, 1986, for a geological map showing these localities). Fig. 6 shows the variation of Fe_2O_3^* , TiO_2 , Zr and Cu with lateral distance. For the most part, the compositional range of these elements lies within the limits of analytical error and highlights the extremely uniform chemical

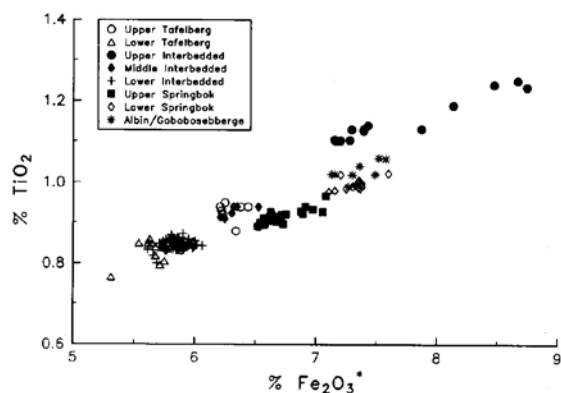


Fig. 7: Plot of TiO_2 against Fe_2O_3^* ; note that in the legend "Interbedded Coastal" subgroups of quartz latites have been abbreviated to "Interbedded".

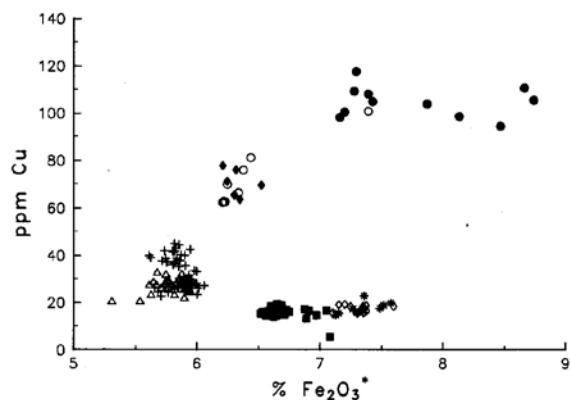


Fig. 8: Plot of Cu against Fe_2O_3^* for the quartz latite units of the Etendeka Formation. See Fig. 7 for legend.

composition of individual quartz latite units.

5. GEOCHEMICAL CORRELATION OF QUARTZ LATITE UNITS

5.1 Compositional Differences

Despite the overall compositional uniformity displayed by the Etendeka quartz latites, small but significant compositional differences do occur between some of the units. The principle discriminating elements are TiO_2 , Fe_2O_3^* and Cu. On the plot of TiO_2 vs. Fe_2O_3^* the Springbok quartz latites can be distinguished from the Tafelberg and Interbedded Coastal groups by relatively higher Fe_2O_3^* content (Fig. 7). The lower and upper Springbok units are not clearly separated on this diagram, although the lower Springbok samples fall at the high TiO_2 and high Fe_2O_3^* end of the lower trend where they are associated with samples from Albin beacon (Erlank *et al.*, 1984) and the Gobobosebberge lava field surrounding the Messum Complex. The lower Tafel-

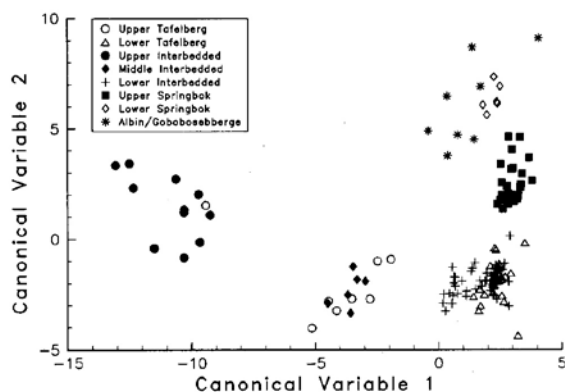


Fig. 9: Discriminant function analysis (DFA) diagram illustrating the maximum possible compositional discrimination between the Tafelberg, Interbedded and Springbok quartz latite units. The formulae for calculating the two canonical variables are given in the Appendix. Note that in the legend "Interbedded Coastal" subgroups of quartz latites have been abbreviated to "Interbedded".

berg and lower Interbedded Coastal quartz latites form a single grouping that can be distinguished from samples of the middle Interbedded Coastal and upper Tafelberg groups. Data for the Upper Interbedded Coastal quartz latites and the Tafelberg Beacon unit plot at the high TiO_2 and Fe_2O_3^* end of the upper trend, forming a cluster of points distinct from the other Tafelberg and Interbedded Coastal quartz latites. It is interesting to note that successive units in the Tafelberg and Interbedded Coastal quartz latites show a trend of increasing Fe_2O_3^* and TiO_2 with increasing stratigraphic height. Quartz latite units within the Springbok group, however, show a decrease in Fe_2O_3^* and TiO_2 with increasing stratigraphic height.

A diagram of Cu vs. Fe_2O_3^* demonstrates the Cu is a more effective discriminant than TiO_2 for the groups discussed so far (Fig. 8). The Springbok quartz latites define a discrete population with a completely different trend to the Tafelberg and Interbedded Coastal groups. Although the lower Interbedded Coastal quartz latites have slightly higher Cu values than those of the lower Tafelberg unit, this plot does not permit a further separation of the Tafelberg and Interbedded Coastal samples from the three groups recognised in Fig. 7.

5.2. Discriminant Function Analysis

The objective of discriminant function analysis (DFA) is to examine how far it is possible to distinguish between members of various groups on the basis of observations made upon them. DFA is a comparative analysis of data which have already been pre-classified into groups using criteria different from those entered in the discriminant function; it is also possible to classify "unknown" samples in terms of the groups defined.

Geochemical data which can be related to different formations or lithological groups, like the quartz latites of the Etendeka, are ideally suited to this type of statistical treatment (Le Maitre, 1982). A full description of the methods employed here can be found in Duncan *et al.* (1984).

A discriminant function is a combination of variables which best describes the inter-group variance of a data set and reduces its dimensionality. In the program used (BMDP7M; Dixon *et al.*, 1981) the variables are chosen in a step-wise selection procedure and entered into the function on the basis of their ability to discriminate between groups. Variables which are strongly correlated with those already in the function are excluded, as they contribute little to increasing the resolving power of the function. The discriminant function is expressed in terms of canonical variables which are a linear combination of weighted variables. The first canonical variable score describes the maximum variance between groups and successive canonical variables the maximum residual variance orthogonal to the previous score. It is important to note that the selection of discriminant elements and the canonical variable scores are

dependent upon the sample groups used in the DFA, and that they change according to the groups used to define the function.

Fig. 9 presents a DFA diagram where all the main quartz latite groups and units were used to define the discriminant function; also plotted are samples from Albin beacon and the Gobosebberge. This diagram is similar in many respects to Fig. 8, however, a distinct separation is observed between the upper and lower Springbok units. The Albin beacon and Gobosebberge samples plot apart from the Lower Springbok samples, a feature not observed on previous diagrams. The separation of the Tafelberg and Interbedded Coastal units into the three groupings recognised in the previous section is not improved.

To increase the discrimination between the Tafelberg and Interbedded Coastal quartz latites, these groups were processed through DFA without the Springbok group (Fig. 10). The lower Tafelberg unit and lower Interbedded Coastal subgroup remain closely associated, although some of the lower Interbedded Coastal samples plot towards the middle Interbedded Coastal subgroup and upper Tafelberg unit. The middle Interbedded Coastal subgroup and upper Tafelberg unit also show a slight separation. In the third cluster of points the single sample from Tafelberg beacon still plots within the upper Interbedded Coastal quartz latite subgroup.

Discriminant functions were also calculated for several combinations of quartz latite group pairs in order to maximise the discrimination between them. The following conclusions were reached from the DFA investigation:

- (1) The upper and lower Springbok units can be discriminated from each other and from the other quartz latite groups.
- (2) Quartz latites from Albin beacon (Erlank *et al.*, 1984) and the Gobosebberge lava field surrounding the Messum Complex are similar to the lower Springbok quartz latites. However, they can be sep-

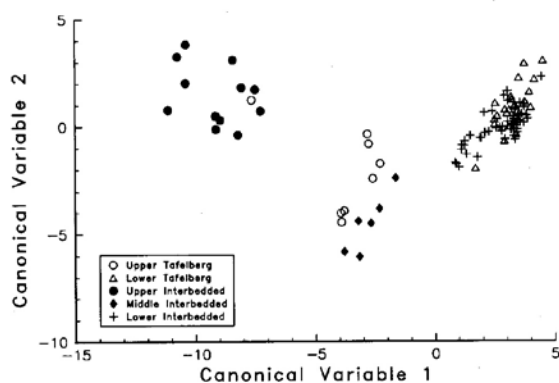


Fig. 10: DFA diagram illustrating the maximum possible compositional discrimination between the Tafelberg and Interbedded Coastal quartz latite units. The formulae for calculating the two canonical variables are given in the Appendix.

arated into a diffuse field of their own when DFA is used to compare them with only the upper and lower Springbok units.

- (3) The "Lower Tafelberg" quartz latites from either side of the Ambrosius Berg Fault Zone are compositionally indistinguishable and represent the same unit.
- (4) The lower Tafelberg middle Tafelberg and Lower Interbedded Coastal quartz latites cannot be discriminated.
- (5) The middle Interbedded Coastal subgroup and upper Tafelberg unit are not significantly different from one another and cannot be discriminated with any degree of confidence.
- (6) The upper Interbedded Coastal quartz latites form a separate group which includes a sample from the Tafelberg beacon unit.

6. STRATIGRAPHIC INTERPRETATION

Based on the correlations discussed above a stratigraphic reconstruction and correlation of the Tafelberg and Interbedded Coastal successions across the southern Etendeka lava field is proposed (Table 2). Because of the different number of quartz latite units encountered in the Tafelberg and Interbedded Coastal sections, the comparison of quartz latite groups in Table 2 is not intended as an absolute correlation of individual units. We suggest that correlated units represent one or more eruptive units from the same 'batch' of quartz latite magma which were deposited over wide areas of the

Etendeka during a particular eruptive cycle.

A schematic section of the Etendeka Formation illustrates the differences in stratigraphy and structure encountered in the eastern and western areas of the Etendeka lava field (Fig. 11a). The main structural break is the Ambrosius Berg Fault Zone (ABFZ). The increasing eastward dip in successive fault blocks to the west of the ABFZ suggests that the faults bounding these blocks are listric in character. Most of the faulting is probably post-volcanic, although some syn-volcanic movements may also have occurred in the period between the eruption of the upper Springbok and lower Tafelberg quartz latite units.

A reconstruction of the Etendeka lava succession, based on the correlations in Table 2, is illustrated in Fig. 11b. The vertical scales on this diagram indicate the approximate thickness of the Tafelberg and Interbedded Coastal sequences, and of the individual units involved (Milner, 1986). Many of the quartz latite units appear to thin and terminate towards the east suggesting that the source area for these quartz latites was in the west.

It is tentatively suggested that the quartz latites from the Albin beacon and the Gobobosebberge lava field form part of the Springbok succession, although a more detailed knowledge of the Gobobosebberge lava suc-

TABLE 2: Stratigraphic correlation of quartz latite units.

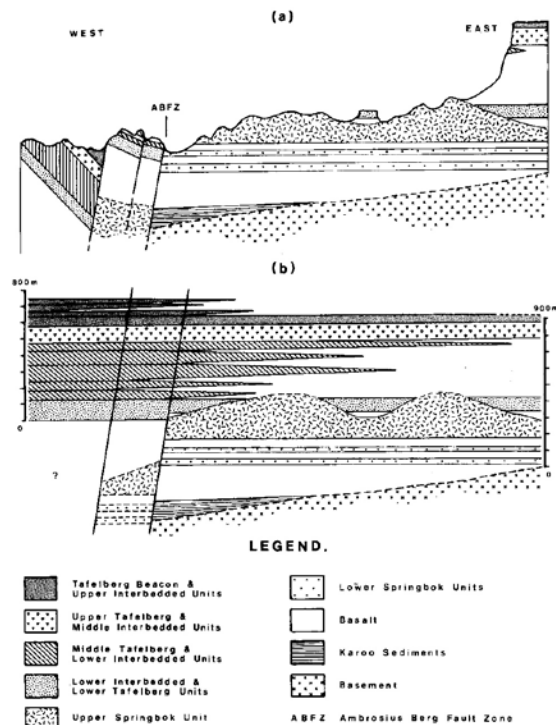
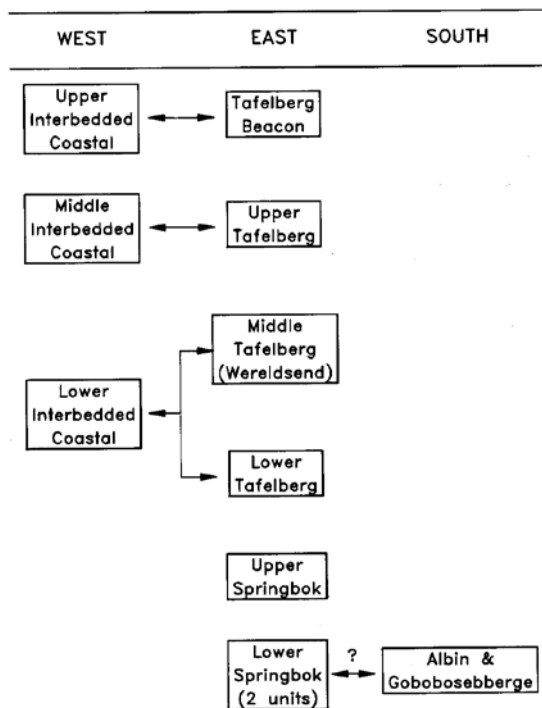


Fig. 11: (a) Schematic cross-section of the Etendeka Formation from Tafelberg (east) to the coast (west). Note that the lower Tafelberg quartz latite is correlated with the basal portion of the lower Interbedded Coastal quartz latite sequence on the basis of petrography. (b) Schematic stratigraphic reconstruction based on (a) but with the effects of post-volcanic faulting removed and without regard to present topography. Note that in the legend "Interbedded Coastal" subgroups of quartz latites have been abbreviated to "Interbedded".

cession and its geochemistry is required to substantiate this.

7. CONCLUSIONS

- (1) Pitchstones and devitrified quartz latites have been affected by secondary alteration. The combination of low concentrations of K_2O and high LOI in the former implies a low temperature hydration event, and an apparent loss of CaO and Na_2O in the latter are related to the alteration of plagioclase.
- (2) The extremely uniform composition displayed by the Etendeka quartz latite units indicates that their magma reservoirs were not compositionally zoned.
- (3) Small, but significant, variations of certain element abundances allow the correlation of quartz latite units across most of the Etendeka area. Discriminant function analysis further enhances our ability to make geochemical correlations.
- (4) A stratigraphic model for the Etendeka Formation is proposed on the basis of these correlations. The thick succession of quartz latites in the west thins and is intercalated with basaltic units in the east. Bellieni *et al.* (1984) have described 200-300 m thick interbedded dacite to rhyolite units in the upper portions of the Serra Geral Formation in the Parana Basin of Brazil. These units are the apparent equivalents of the Etendeka quartz latites in a pre-drift Gondwanaland reconstruction, although no direct geochemical correlation with the units described by Bellieni *et al.* (1984) can be attempted until possible inter-laboratory analytical variations have been assessed.

8. ACKNOWLEDGEMENTS

We owe particular thanks to Roy Miller for his earlier mapping of the Etendeka Formation and for many hours of fruitful discussion in the field. We have also benefited greatly from discussions with Tony Erlank, Goonie Marsh and the late Peter Betton. Our work in the Etendeka area has been supported by a grant from the SWA/Namibia Committee for Research Priorities (CRP). We acknowledge thorough and constructive reviews of the manuscript by Roger Scoon and Brian Hoal.

9. REFERENCES

- Bellieni, G., Brotzu, P., Comin-Chiaramonti, P., Ernesto, M., Melfi, A., Pacca, I.G. and Piccirillo, E.M. 1984. Flood basalt to rhyolite suites in the southern Parana Plateau (Brazil): Palaeomagnetism, petrogenesis and geochemical implications. *J. Petrol.*, **25**, 579-618.
- Cerling, T.E., Brown, F.H. and Bowman, J.R. 1985. Low-temperature alteration of volcanic glass: Hydration, Na, $K^{18}O$ and Ar mobility. *Chem. Geol.*, **52**, 281-293.
- Dixon, W.J., Brown, M.B., Engelman, L., Frane, J.W., Hill, M.A., Jennrich, R.I. and Toporek, J.D. 1981. *BMDP statistical software*. Univ. of California Press, Berkeley, 785 pp.
- Duncan, A.R., Erlank, A.J. and Marsh, J.S. 1984. Regional geochemistry of the Karoo Igneous Province. *Spec. Publ. geol. Soc. S. Afr.*, **13**, 355-388.
- Erlank, A.J., Marsh, J.S., Duncan, A.R., Miller, R.McG., Hawkesworth, C.J., Betton, P.J. and Rex, D.C. 1984. Geochemistry and petrogenesis of the Etendeka volcanic rocks from S.W.A./Namibia. *Spec. Publ. geol. Soc. S. Afr.*, **13**, 195-245.
- Hildreth, W. 1979. The Bishop Tuff: evidence for the origin of compositional zonation in magma chambers. *Spec. publ. geol. Soc. Am.*, **180**, 43-75.
- Hildreth, W. 1981. Gradients in silicic magma chambers: implications for lithospheric magmatism. *J. geophys. Res.*, **86**, 10153-10192.
- Jezek, P.A. and Noble, D.C. 1978. Natural hydration and ion exchange of obsidian: an electron microprobe study. *Am. Miner.*, **63**, 266-273.
- Le Maitre, R.W. 1982. *Numerical Petrology*. Elsevier, 281 pp.
- Mackenzie, D.E. and Chappell, B.W. 1972. Shoshonitic and calc-alkaline lavas from the highlands of Papua New Guinea. *Contrib. Mineral. Petrol.*, **35**, 50-62.
- Milner, S.C. 1986. The geological and volcanological features of the quartz latites of the Etendeka Formation. *Communs geol. Surv. S.W. Africa/Namibia*, **2**, 109-116.
- Peccerillo, A. and Taylor, S.R. 1976. Geochemistry of Eocene calc-alkaline volcanic rocks from the Kastamonu area northern Turkey. *Contrib. Mineral. Petrol.*, **58**, 63-81.
- Ritchey, J.L. 1980. Divergent magmas at Crater Lake, Oregon: products of fractional crystallisation and vertical zoning in a shallow, water-undersaturated chamber. *J. Volcan. Geotherm. Res.*, **7**, 373-386.
- Smith, R.L. and Bailey, R.A. 1966. The Bandelier Tuff: a study of ash flow eruption cycles from zoned magma chambers. *Bull. volcan.*, **29**, 83-104.
- Smith, R.L. 1979. Ash flow magmatism. *Spec. Publ. geol. Soc. Am.*, **180**, 5-27.
- Williams, H. 1942. The geology of Crater Lake National Park. *Carnegie Instn. Wash. Publ.*, **540**, 1-162.
- Zielinski, R.A. 1982. The mobility of uranium and other elements during alteration of rhyolite ash to montmorillonite: a case study in the Troublesome Formation, Colorado, U.S.A. *Chem. geol.*, **35**, 185-204.

APPENDIX

The canonical variable scores are calculated according to the equations given below. Major oxide concentrations were expressed in weight % and trace element concentrations in ppm, the data were not normalised to 100% on a volatile-free basis prior to calculating canonical variable (CV) scores.

Fig. 9:

$$\begin{aligned} \text{CV1} &= -(\text{TiO}_2 * 27.952) + (\text{Al}_2\text{O}_3 * 0.41343) + (\text{Fe}_2\text{O}_3 * 1.0670) \\ &\quad - (\text{P}_2\text{O}_5 * 14.870) + (\text{Ba} * 0.00458) + (\text{Zr} * 0.05536) \\ &\quad - (\text{Cu} * 0.08252) + 3.3561 \\ \text{CV2} &= -(\text{TiO}_2 * 2.3059) - (\text{Al}_2\text{O}_3 * 0.35222) + (\text{Fe}_2\text{O}_3 * 3.1557) \\ &\quad - (\text{P}_2\text{O}_5 * 46.007) + (\text{Ba} * 0.00435) + (\text{Zr} * 0.12755) \\ &\quad - (\text{Cu} * 0.02577) - 36.302 \end{aligned}$$

Fig. 10:

$$\begin{aligned} \text{CV1} &= -(\text{TiO}_2 * 21.337) + (\text{Al}_2\text{O}_3 * 1.1980) + (\text{Ba} * 0.00036) \\ &\quad + (\text{Nb} * 0.18515) - (\text{V} * 0.04694) - (\text{Cu} * 0.07132) + \\ &\quad (\text{Y} * 0.10051) + 1.8007 \\ \text{CV2} &= +(\text{TiO}_2 * 14.657) - (\text{Al}_2\text{O}_3 * 2.6432) + (\text{Ba} * 0.00754) \\ &\quad + (\text{Nb} * 0.85879) - (\text{V} * 0.12429) - (\text{Cu} * 0.03202) + \\ &\quad (\text{Y} * 0.01077) + 4.1757 \end{aligned}$$